Optics and Photonics Journal, 2012, 2, 260-264
http://dx.doi.org/10.4236/opj.2012.24031 Published Online December 2012 (http://www.SciRP.org/journal/opj)

Phase-Matching and Parametric Conversion for the Mid-Infrared in As_2S_3 Waveguides

Qi Chen, Xin Wang, Christi Madsen
Department of Electrical & Computer Engineering, Texas A&M University, College Station, USA
Email: chenqicage21@neo.tamu.edu

Received September 7, 2012; revised October 5, 2012; accepted October 17, 2012

ABSTRACT

We illustrate two As_2S_3 waveguide designs for four-wave mixing, which can generate 3.03 μm mid-infrared light from a 1.55 μm near-infrared signal source and a 2.05 μm pump source. Through simulations, we verify that four-wave mixing phase-matching efficiencies up to 100% can be achieved using dispersion engineering to maintain the dispersion at 2.05 μm near to zero. The best conversion efficiency is –10 dB. When the waveguide length is 1 cm, the parametric conversion bandwidth is 1525 nm. We also evaluated the shift of 100% phase-matching efficiency wavelengths based upon fabrication tolerances.

Keywords: As_2S_3; Mid-Infrared; Phase-Matching; Four-Wave Mixing

1. Introduction

Four-wave mixing (FWM) is a third-order nonlinear process. In degenerate FWM, if the phase-matching condition is met, two pump photons and a signal photon can generate an idler photon. In mid-infrared (Mid-IR) region, the vast majority of gaseous chemical substances exhibit fundamental vibrational absorption bands, and the absorption of light provides a nearly universal means for their detection [1]. The high sensitivity and capability of non-intrusive *in-situ* detection make it ideal for trace gas detection.

Recently, although many papers have been published on FWM in silicon waveguides for both near-infrared (near-IR) [2-9] and mid-IR [10,11] and in chalcogenide waveguides for near-IR [12-14], the parametric conversion by FWM for mid-IR in chalcogenide waveguides has not been demonstrated yet. In addition, the applications silicon waveguides cannot be utilized over 2.5 μm wavelength region due to the strong absorption from the substrate material, silicon dioxide (SiO_2). On the contrary, lithium niobate ($LiNbO_3$), as a widely-used optical material, has very high transmission over the wavelength range from 0.42 to 5.2 μm and exhibits excellent electro-optic, nonlinear and piezoelectric properties. Therefore, it is a good substrate material for mid-IR integrated optics up to 5 μm.

Chalcogenide glasses have been investigated as an alternative platform for nonlinear signal processing [15]. They are a set of amorphous materials which show good transparency and low loss for both 1.3 μm - 1.55 μm telecommunication windows and into the mid-IR region. Arsenic tri-sulfide (As_2S_3) is very popular among them by its low two photon absorption (TPA) coefficient, which makes it ideal for nonlinear optics. Magnesium fluoride (MgF_2), which has wide transmission range (0.2 μm - 7 μm) into the mid-IR, is a good candidate for cladding material because of its lower refractive index. Magnesium fluoride (MgF_2), which has wide transmission range (0.2 μm - 7 μm) at mid-IR, is a good candidate for cladding material because of its ruggedness and durability. It also keeps the potential of optical tuning by adding electrodes on it.

In this paper, we report two As_2S_3 waveguide designs, which have near zero dispersion at a pump wavelength of 2.05 μm and satisfy the phase-matching condition at a signal wavelength of 1.55 μm. The corresponding idler wavelength is 3.03 μm which is a common operation wavelength for trace gas sensors [16]. The FWM phase-matching efficiency can be as high as 100%. Through simulations, we verify that the parametric conversion efficiency is –10 dB for pump power intensity of 0.1 GW/cm^2. Under the same intensities, our results are 20 dB better than the parametric conversion efficiency of silicon waveguides.

2. Dispersion Engineering

To satisfy the phase-matching condition, dispersion engineering is required. In the first place, we have to maintain the very low dispersion at the pump wavelength by varying the waveguide dimensions. To achieve high effi-

cient FWM, it is also necessary to tune the 100% phase-matching efficiency at signal wavelength by changing cladding thickness. **Figures 1(a)** and **(b)** show that the structures of As_2S_3 waveguide with and without MgF_2 top cladding. The reason to simulate different designs is to evaluate the influence of MgF_2 on conversion bandwidth.

The resulting dispersion curves for the fundamental TE mode are demonstrated in **Figure 2**. All simulations are from Fimmwave, a commercial software by Photo Design Inc. When the waveguide width is 1.4 μm and the height is 1.7 μm with 0.18 μm MgF_2 cladding on top of it, the dispersion at 2.05 μm is 1.2 ps/nm/km which is very close to zero; when the waveguide width is 1.5 μm and the height is 1.685 μm without a cladding material, the zero dispersion wavelength is exactly 2.05 μm.

3. Phase-Matching Condition and FWM Phase-Matching Efficiency

FWM is a nonlinear phase-matched process resulting from the near-instantaneous third-order susceptibility, $\chi^{(3)}$ [17]. For degenerate FWM, the relationship of the three wavelengths can be described as:

$$\frac{1}{\lambda_i}=\frac{2}{\lambda_p}-\frac{1}{\lambda_s} \tag{2}$$

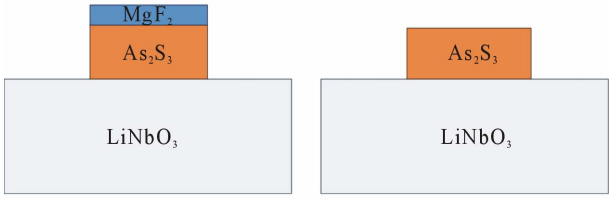

Figure 1. (a) As_2S_3 waveguide with MgF_2 cladding (b) without cladding.

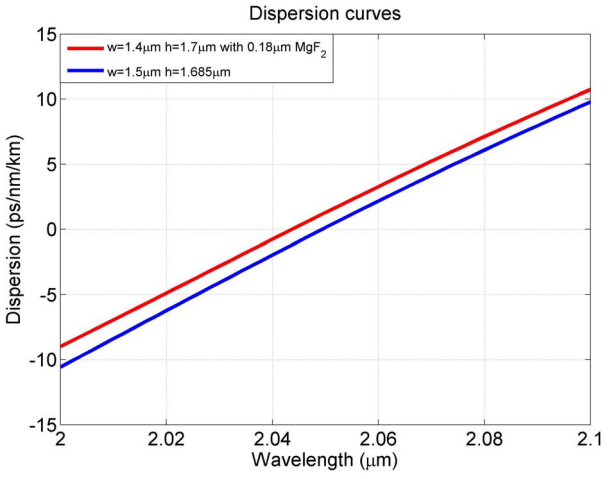

Figure 2. Dispersion curves for two As2S3 waveguide designs.

where λ_i, λ_p and λ_s are idler, pump and signal wavelengths. The FWM phase-matching efficiency depends on how well the phase-matching condition is satisfied:
where n_s, n_i and n_p are effective indices of signal, idler and pump wavelengths; P_p is pump power.

$$\Delta\kappa=2\pi\left(\frac{n_s}{\lambda_s}+\frac{n_i}{\lambda_i}-2\frac{n_p}{\lambda_p}\right)+2\gamma P_p \tag{2}$$

$$\gamma=\frac{2\pi n_2}{\lambda_p A_{eff}} \tag{3}$$

γ is nonlinearity coefficient. A_{eff} is effective mode area for the pump, which are 1.84 μm^2 and 1.99 μm^2 for the structures with and without MgF_2 cladding, respectively.

If the phase-matching condition is achieved, the FWM efficiency can be very high. It is described by the following formula in [18]:

$$\eta^2=\frac{{\alpha_0}^2}{{\alpha_0}^2+\Delta\kappa^2}\left[1+4\mathrm{e}^{-\alpha_0 L}\frac{\sin^2\left(L\Delta\kappa/2\right)}{\left(1-\mathrm{e}^{-\alpha_0 L}\right)^2}\right] \tag{4}$$

where α_0 is the waveguide propagation loss at 2.05 μm. We use a value of 0.33 dB/cm from our previous work [19]. Since TPA coefficient of As_2S_3 is very small, the nonlinear loss due to it can be neglected. L is the length of As_2S_3 waveguide, 4 cm.

Figure 3 shows the phase-matching curves for the two As_2S_3 waveguide designs. The phase-matching condition is met at 1.55 μm, 3.03 μm and the region near the pump wavelength, which means that the FWM phase-matching efficiency, depicted in **Figure 4**, can be as high as 100% at these wavelengths for both designs. In wavelength regions near 1.55 and 3.03 μm, the FWHM of the structure without cladding is 25 nm, which is 9 nm wider than that of structure with MgF_2 cladding on top.

4. Coupled Equation and Parametric Conversion Efficiency

FWM can be described by the following coupled differential equations [20]:

$$\frac{\partial A_s}{\partial z}=\mathrm{i}\gamma\left(\left|A_s\right|^2+2\left|A_i\right|^2+2\left|A_p\right|^2\right)A_s +\gamma A_p^2 A_i^* \exp\left(-\mathrm{i}\Delta\kappa z\right) \tag{5}$$

$$\frac{\partial A_i}{\partial z}=\mathrm{i}\gamma\left(\left|A_i\right|^2+2\left|A_s\right|^2+2\left|A_p\right|^2\right)A_i +\gamma A_p^2 A_s^* \exp\left(-\mathrm{i}\Delta\kappa z\right) \tag{6}$$

$$\frac{\partial A_p}{\partial z}=\mathrm{i}\gamma\left(\left|A_p\right|^2+2\left|A_i\right|^2+2\left|A_s\right|^2\right)A_p +2\gamma A_i A_s A_p^* \exp\left(\mathrm{i}\Delta\kappa z\right) \tag{7}$$

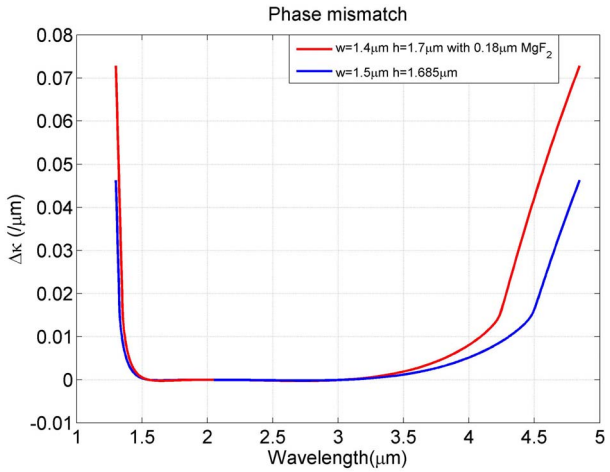

(a)

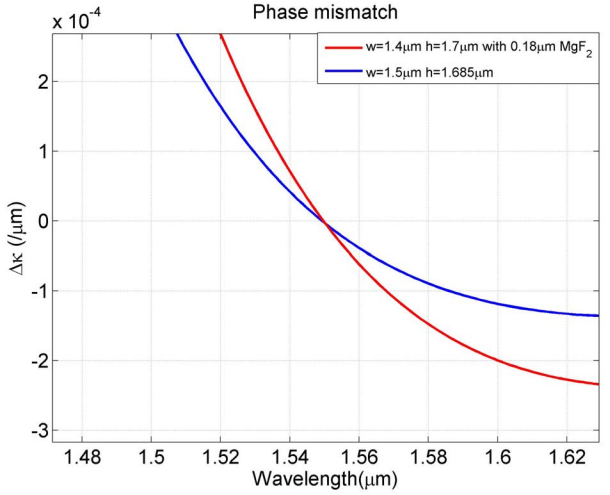

(b)

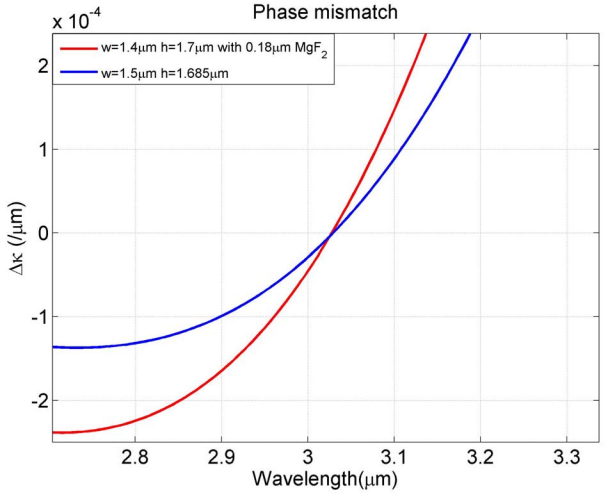

(c)

Figure 3. (a) Phase mismatch curves as a function of signal wavelength; (b) Phase mismatch around 1.55 μm and (c) 3.03 μm.

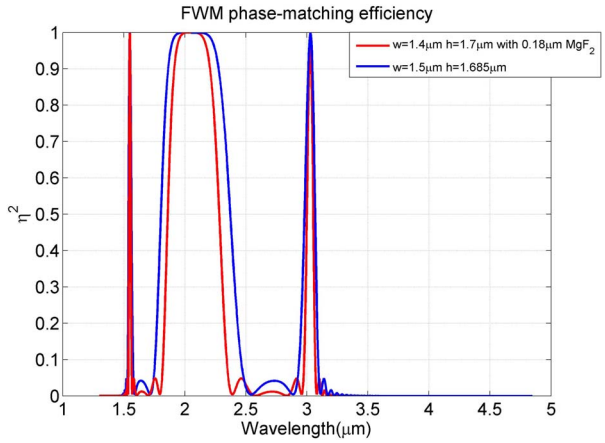

Figure 4. FWM phase-matching efficiency as a function of signal wavelength.

where A_p, A_s and A_i denote the complex electric field amplitude of pump, signal and idler wavelengths, respectively. An improved understanding can be obtained by considering a strong pump and a weak signal incident such that the pump remains undepleted during the FWM process [20]. Therefore, the coupled differential equations can be solved by an analytic method. The parametric conversion efficiency is described by:

$$G_i = \left[\frac{\gamma P_p}{g}\sinh\left(gL_{eff}\right)\right]^2 \tag{9}$$

where g is parametric gain and L_{eff} is the effective As_2S_3 waveguide length for nonlinear process. They can be expressed by:

$$g = \sqrt{\left(\gamma P_p\right)^2 - \left(\Delta\kappa/2\right)^2}$$

For simulation purposes, the pump power intensity coupled into the As_2S_3 waveguide are chosen to be 0.1 GW/cm^2 and 0.01 GW/cm^2, respectively. The parametric conversion

$$L_{eff} = \frac{1-\exp\left(-\alpha_0 L\right)}{\alpha_0} \tag{10}$$

efficiency G_i is shown in **Figure 5**. When L is 4 cm, G_i is –10 dB and –30 dB for each pump power intensity. Under the same intensities, our results are 20 dB better than the parametric conversion efficiency of silicon waveguides in [21]. The remarkable improvement is mainly due to the 100% FWM phase-matching efficiency η^2.

5. Fabrication Tolerance

In addition to the high nonlinearity, chalcogenide glass exhibits photosensitivity, too [22]. We have studied the photodarkening effect of As_2S_3 in a hybrid Mach-Zehnder interferometer [23]. A uniform exposure to

intensive green light can increase As_2S_3 refractive index by 1% [5], which can change the phase-matching condition of the As_2S_3 waveguides. It provides the tuning ability after traditional photolithography.

Figure 6 shows that the FWM phase-matching efficiency curves for the design with MgF_2 cladding when the refractive index of As_2S_3, waveguide width or height is changed. These cases may happen during fabrication. The changes shift the 100% phase-matching efficiency wavelengths, which are summarized in **Table 1**.

Figure 7 demonstrates the parametric conversion efficiency curves corresponding to the different As_2S_3 waveguide lengths for 0.1 GW/cm^2 pump power intensity. Due to the length dependence of phase-matching ($L\Delta\kappa$), the conversion bandwidth increases with the decreasing waveguide length. When L is 1 cm (L_{eff} = 0.96 cm), the conversion bandwidth is 1525 nm corresponding to –21 dB parametric conversion efficiency. The flat curve indicates that we can achieve continuously tunable

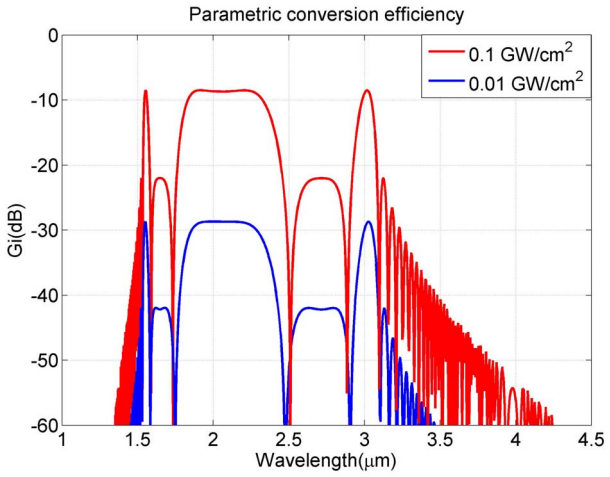

Figure 5. Parametric conversion efficiency as a function of signal wavelength.

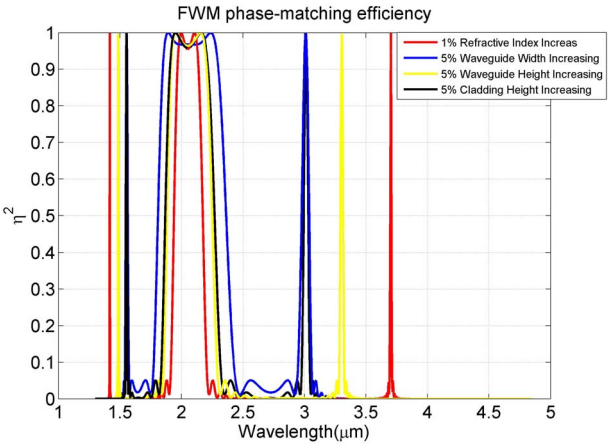

Figure 6. FWM phase-mismatch efficiency as a function of signal wavelength.

Table 1. 100% FWM phase-matching efficiency wavelengths for different fabrication tolerances.

Fabrication tolerances	100% FWM phase-matching efficiency wavelength (μm)	Idler wave length (μm)
1% refractive index increasing of As_2S_3	1.418	3.698
5% waveguide width increasing	1.555	3.007
5% waveguide height increasing	1.486	3.304
5% cladding height increasing	1.554	3.013

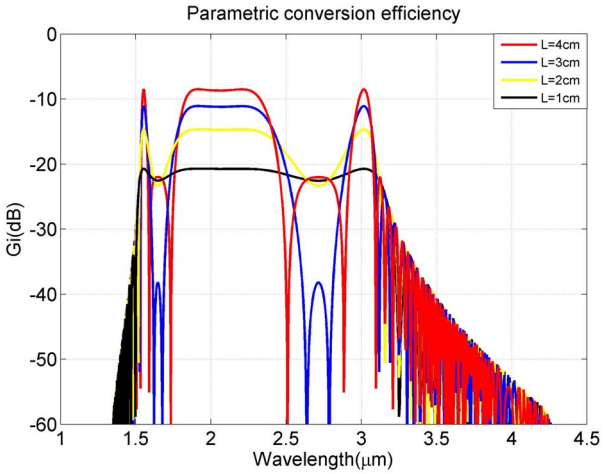

Figure 7. Parametric conversion efficiency as a function of signal wavelength.

FWM between the near-IR and mid-IR.

6. Conclusion

In this paper, we presented mid-IR FWM simulations for As_2S_3 waveguides, which can generate 3.03 μm mid-IR light by a 1.55 μm near-IR signal source and a 2.05 μm pump source. The FWM phase-matching efficiency at 1.55 μm is up to 100% for the designs with and without MgF_2 cladding. For 0.1 GW/cm^2 pump power intensity, the best parametric conversion efficiency at 3.03 μm is –10 dB, which is 20 dB better than the results in silicon waveguides in [21]. The largest conversion bandwidth of 1525 nm is achieved when the waveguide length is 1 cm. In addition, we simulated the 100% FWM phase-matching efficiency shift for various fabrication variations.

7. Acknowledgements

This material is based upon work supported by the National Science Foundation under grant No. EEC-0540832.

REFERENCES

[1] F. Tittel, D. Richter and A. Fried, "Mid-Infrared Laser Applications in Spectroscopy," *Solid-State Mid-Infrared Laser Sources*, 2003, pp. 458-529.

[2] M. A. Foster, A. C. Turner, J. E. Sharping, B. S. Schmidt, M. Lipson and A. L. Gaeta, "Broad-Band Optical Parametric Gain on a Silicon Photonic Chip," *Nature*, Vol. 441, No. 7096, 2006, pp. 960-963. doi:10.1038/nature04932

[3] Q. Lin, J. D. Zhang, P. M. Fauchet and G. P. Agrawal, "Ultrabroadband Parametric Generation and Wavelength Conversion in Silicon Waveguides," *Optics Express*, Vol. 14, No. 11, 2006, pp. 4786-4799. doi:10.1364/OE.14.004786

[4] A. C. Turner, C. Manolatou, B. S. Schmidt, M. Lipson, M. A. Foster, J. E. Sharping and A. L. Gaeta, "Tailored Anomalous Group-Velocity Dispersion in Silicon Channel Waveguides," *Optics Express*, Vol. 14, No. 10, 2006, pp. 4357-4362. doi:10.1364/OE.14.004357

[5] D. Dimitropoulos, V. Raghunathan, R. Claps and B. Jalali, "Phase-Matching and Nonlinear Optical Processes in Silicon Waveguides," *Optics Express*, Vol. 12, No. 1, 2004, pp. 149-160. http://www.opticsinfobase.org/abstract.cfm?URI=oe-12-1-149 doi:10.1364/OPEX.12.000149

[6] V. Raghunathan, R. Claps, D. Dimitropoulos and B. Jalali, "Parametric Raman Wavelength Conversion in Scaled Silicon Waveguides," *Journal of Lightwave Technology*, Vol. 23, No. 6, 2005, pp. 2094-2102. doi:10.1109/JLT.2005.849895

[7] H. Fukuda, K. Yamada, T. Shoji, M. Takahashi, T. Tsuchizawa, T. Watanabe, J. Takahashi and S. Itabashi, "Four-Wave Mixing in Silicon Wire Waveguides," *Optics Express*, Vol. 13, No. 12, 2005, pp. 4629-4637. http://www.opticsinfobase.org/abstract.cfm?URI=oe-13-12-4629 doi:10.1364/OPEX.13.004629

[8] K. Yamada, H. Fukuda, T. Tsuchizawa, T. Watanabe, T. Shoji and S. Itabashi, "All-Optical Efficient Wavelength Conversion Using Silicon Photonic Wire Waveguide," *IEEE Photonics Technology Letters*, Vol. 18, No. 9, 2006, pp. 1046-1048. doi:10.1109/LPT.2006.873469

[9] M. A. Foster, A. C. Turner, R. Salem, M. Lipson and A. L. Gaeta, "Broad-Band Continuous-Wave Parametric Wavelength Conversion in Silicon Nanowaveguides," *Optics Express*, Vol. 15, No. 20, 2007, pp. 12949-12958. http://www.opticsinfobase.org/oe/abstract.cfm?URI=oe-15-20-12949 doi:10.1364/OE.15.012949

[10] S. Zlatanovic, J. S. Park, S. Moro, J. M. Chavez Boggio, I. B. Divliansky, N. Alic, S. Mookherjea and S. Radic, "Mid-Infrared Wavelength Conversion in Silicon Waveguides Using Ultracompact Telecom-Band-Derived Pump Source," *Nature Photonics*, Vol. 4, No. 8, 2010, pp. 561-564. doi:10.1038/nphoton.2010.117

[11] X. Liu, R. M. Osgood Jr, Y. A. Vlasov and W. M. J. Green, "Mid-Infrared Optical Parametric Amplifier Using Silicon Nanophotonic Waveguides," *Nature Photonics*, Vol. 4, No. 8, 2010, pp. 557-560. doi:10.1038/nphoton.2010.119

[12] R. Ahmad and M. Rochette, "Chalcogenide Optical Parametric Oscillator," *Optics Express*, Vol. 20, No. 9, 2012, pp. 10095-10099. doi:10.1364/OE.20.010095

[13] R. Ahmad and M. Rochette, "High Efficiency and Ultra Broadband Optical Parametric Four-Wave Mixing in Chalcogenide-PMMA Hybrid Microwires," *Optics Express*, Vol. 20, No. 9, 2012, pp. 9572-9580. doi:10.1364/OE.20.009572

[14] D. Yeom, E. Mägi, M. Lamont, M. Roelens, L. Fu and B. Eggleton, "Low-Threshold Supercontinuum Generation in Highly Nonlinear Chalcogenide Nanowires," *Optics Letters*, Vol. 33, No. 7, 2008, pp. 660-662. doi:10.1364/OL.33.000660

[15] M. Asobe, "Nonlinear Optical Properties of Chalcogenide Glass Fibers and Their Application to All-Optical Switching," *Optical Fiber Technology*, Vol. 3, No. 2, 1997, pp. 142-148. doi:10.1006/ofte.1997.0214

[16] A. Bohren and M. W. Sigrist, "Optical Parametric Oscillator Based Difference Frequency Laser Source for Photoacoustic Trace Gas Spectroscopy in the 3-µm midIR Range," *Infrared Physics & Technology*, Vol. 38, No. 7, 1997, pp. 423-435. doi:10.1016/S1350-4495(97)00041-8

[17] G. P. Agrawal, "Nonlinear Fiber Optics," Academic Press, San Diego, 2001, Chapter 10.

[18] T. Vallaitis, S. Bogatscher, L. Alloatti, P. Dumon, R. Baets, M. L. Scimeca, I. Biaggio, F. Diederich, C. Koos, W. Freude and J. Leuthold, "Optical Properties of Highly Nonlinear Silicon-Organic Hybrid (SOH) Waveguide Geometries," *Optics Express*, Vol. 17, No. 20, 2009, pp. 17357-17368. doi:10.1364/OE.17.017357

[19] X. Xia, Q. Chen, C. Tsay, C. B. Arnold and C. K. Madsen "Low-Loss Chalcogenide Waveguides on Lithium Niobate for the Mid-Infrared," *Optics Letters*, Vol. 35, No. 19, 2010, pp. 3228-3230. doi:10.1364/OL.35.003228

[20] J. Hansryd, P. A. Andrekson, M. Westlund, L. Jie and P. O. Hedekvist, "Fiber-Based Optical Parametric Amplifiers and Their Applications," *IEEE Journal of Selected Topics in Quantum Electronics*, Vol. 8, No. 3, 2002, pp. 506-520. doi:10.1109/JSTQE.2002.1016354

[21] E.-K. Tien, Y. W. Huang, S. M. Gao, Q. Song, F. Qian, S. K. Kalyoncu and O. Boyraz, "Discrete Parametric Band Conversion in Silicon for Mid-Infrared Applications," *Optics Express*, Vol. 18, No. 21, 2010, pp. 21981-21989. doi:10.1364/OE.18.021981

[22] M. R. Lamont, B. Luther-Davies, D.-Y. Choi, S. Madden, X. Gai and B. J. Eggleton, "Net-Gain from a Parametric Amplifier on a Chalcogenide Optical Chip," *Optics Express*, Vol. 16, No. 25, 2008, pp. 20374-20381. doi:10.1364/OE.16.020374

[23] W. C. Tan, Q. Chen, J. H. Kim and C. Madsen, "A Hybrid As2S3 Mach-Zehnder Interferometer Prepared by Magnetron Sputtering and Its Photodarkening Effect," *IEEE Journal of Quantum Electronics*, Vol. 48, No. 2, 2011, pp. 237-243.

